Chemical Engineering Journal 174 (2011) 595–602

Contents lists available at SciVerse ScienceDirect

Chemical Engineering Journal

journal homepage: www.elsevier.com/locate/cej

# Evaluating the photodegradation of Carbamazepine in a sequential batch photoreactor system: Impacts of effluent organic matter and inorganic ions

Meng Nan Chong[a,b,c,*], Bo Jin[b,c,**], Giuseppe Laera[c,e], Christopher P. Saint[d]

[a] CSIRO Land and Water, Ecosciences Precinct, Dutton Park, Queensland 4102, Australia
[b] School of Chemical Engineering, The University of Adelaide, Adelaide, SA 5005, Australia
[c] School of Earth and Environmental Sciences, The University of Adelaide, Adelaide, SA 5005, Australia
[d] SA Water Centre for Water Management and Re-use, University of South Australia, Mawson Lakes, SA 5095, Australia
[e] Istituto di Ricerca Sulle Acque CNR, Viale F. De Blasio 5, Bari, Italy

ARTICLE INFO

*Article history:*
Received 12 July 2011
Received in revised form 9 September 2011
Accepted 12 September 2011

*Keywords:*
$TiO_2$
Kaolinite
Annular reactor
Photocatalysis
Municipal wastewater

ABSTRACT

Removal of pharmaceutical Carbamazepine (CBZ) compound from municipal wastewater has become an issue from the human health and environmental risks point of view, due to its latent recalcitrance and toxicity properties. This study investigated the photodegradation performance of a sequential batch annular slurry photoreactor (SB-ASP) system for the removal of CBZ compound from secondary municipal wastewater. Two different immobilised $TiO_2$ photocatalysts, namely anatase titanate nanofiber and mesoporous $TiO_2$ impregnated kaolinite catalyst were applied in the SB-ASP system. Various modes of sequential batch reactor (SBR) cycles, presence of effluent organic matter (EOM) and inorganic ions, mainly nitrate and phosphate that could affect the photodegradation performance of the SB-ASP system were evaluated during the removal of CBZ. High performance size exclusion chromatography revealed that the photocatalytic reaction will preferentially compete and attack on high molecular weight EOM prior to the photodegradation of CBZ. The presence of inorganic ions was found to affect the surface fouling of immobilised photocatalysts used to a different extent, without completely retarding their photoactivity. This study also highlighted that the operation of SB-ASP system was useful to enhance the photodegradation of CBZ compound in a semi-continuous operation without constant catalyst replacement. It is foreseeable that the integration of SB-ASP system with biological treatment systems could provide an advanced treatment option for the recycling and reuse of municipal wastewater.


## 1. Introduction

In recent years, the presence of pharmaceutical residues in wastewater has drawn an increasing attention from research institutions and government organisations to public community worldwide, owing to their potential deleterious impacts on human beings and natural ecosystems [1,2]. When the pharmaceutical drugs are consumed, a proportion of these compounds remains unchanged and passes through the human bodies as metabolites into the sewage system [3–5]. Muir et al. [6] reported that 56–68% of a particular pharmaceutical compound can be excreted from the body during therapeutic use. Owing to the high chemical stability and recalcitrant characteristics of these compounds, they are usually found in the environment (or water) because of the removal limitation of current wastewater treatment plants (WWTPs). This has caused the residual pharmaceutical compounds to be transported to natural ecosystem and causing possible contamination to groundwater, surface water as well as drinking water sources [6–11]. Such an indirect route of pharmaceuticals discharge has created significant potential risks to human health and

*Abbreviations:* AMW, apparent molecular weight; AOPs, advanced oxidation processes; AR, analytical reagent; ASP, annular slurry photoreactor; °C, celsius; C, carbon; CBZ, Carbamazepine; cm, centimeter; COD, chemical oxygen demand; $Cr^{3+}$, chromium ions; d, day; Da, Dalton; DO, dissolved oxygen; EOM, effluent organic matter; Fig., figure; g, gram; h, hour; $H^+$, hydrogen ions; HCl, hydrochloric acid; $HNO_3$, nitric acid; HPLC, high performance liquid chromatography; HPSEC, high performance size exclusion chromatography; K, kaolinite; $K_2Cr_2O_7$, potassium dichromate; kDa, kilo-Dalton; L, liter; M, molar; $m^2$, square meter; MBR, membrane bioreactor; min, minute; mL, milliliter; mM, millimolar; MW cm, molecular weight; MΩ cm, milli-Ohm-centimeter; N, nitrogen; NaOH, sodium hydroxide; nm, nanometer; $NO_3^-$, nitrate; P, phosphorus; $PO_4^{3-}$, phosphate; PTPE, polytetrapropylene; SB-ASP, sequential batch annular slurry photoreactor; SBR, sequential batch reactor; SRT, sludge retention time; $TiO_2$, titanium dioxide; $TiO_2$–K, mesoporous titanium dioxide–kaolinite; TNC, anatase titanate nanofiber catalyst; UV, ultraviolet; UVC, ultraviolet-C; μm, micrometer; Vis, visible; W, watt; w/v, weight to volume; WWTP, wastewater treatment plant.

* Corresponding author at: CSIRO Land and Water, Ecosciences Precinct, Dutton Park, Queensland 4102, Australia. Tel.: +61 7 3833 5593; fax: +61 7 3833 5501.
** Corresponding author at: School of Earth and Environmental Sciences, The University of Adelaide, SA 5005, Australia. Tel: +61 8 8303 7056; fax: +61 8 8303 6222.
*E-mail addresses:* meng.chong@csiro.au (M.N. Chong), bo.jin@adelaide.edu.au (B. Jin).

1385-8947/$ – see front matter © 2011 Elsevier B.V. All rights reserved.
doi:10.1016/j.cej.2011.09.065

environment. Therefore, there is a need for a better sewage treatment technology that could remove these residual contaminants from wastewater effluents and prevents their adverse effects from deteriorating human health and natural environments.

Recently, the needs for advanced wastewater treatment technologies are becoming more eminent when the treated effluent is to be recycled for non-potable end-uses (e.g. toilet flushing, clothes washing and garden irrigation). This is due to the higher possibility for potential human contacts or ingestion that may cause severe chemical chronic risk exposures. Radjenović et al. [12] reported that the degree of biotransformation for 31 pharmaceuticals in advanced membrane bioreactor (MBR) system is better than in conventional activated sludge treatment process. However, they found that a few pharmaceuticals such as loratidine, Carbamazepine (CBZ) and hydrochlorothiazide were not removed in the MBR system even at a higher sludge retention time. Other advanced treatment technologies such as ozonation, ultraviolet (UV) irradiation, photo-Fenton and filtration with granular activated carbon have also been assessed for their treatment effectiveness in the removal of these pharmaceutical compounds [13–15]. Results showed that all of these advanced treatment methods demonstrated a treatment limitation towards the removal of pharmaceutical compounds from wastewater, to a certain extent, without completely eliminating them from the source waters. In addition, most of these advanced treatment technologies incurred a higher treatment cost and creates secondary pollution as the pharmaceutical residuals is transferred from one phase (liquid) to another (solid) rather than being completely eliminated. To overcome these shortcomings, different combinations of treatment technologies were made such as adsorption with ozonation or MBR with various advanced oxidation processes (AOPs) to improve the degree of pharmaceuticals removal in wastewater [14–16].

Among the AOPs, heterogeneous photocatalysis employing semiconductor titanium dioxide ($TiO_2$) is an attractive alternative which can be integrated with biological treatment process and other AOPs [14,17–19]. The mechanisms for the formation of electron-hole pairs on surface of $TiO_2$ particles via a series of redox reactions are well-documented [20]. When the $TiO_2$ is photon-activated, the intermediary-formed hydroxyl radicals can react indiscriminately on any pharmaceutical compounds in order to degrade or even complete mineralisation. In this instance, the $TiO_2$ photocatalysis could be integrated as a post-treatment process after the secondary biological wastewater treatment stage [19]. The treated effluent can be recycled back to biological process so as to enhance the biotransformation process for pharmaceutical compounds. To date, the commercial application of $TiO_2$ photocatalysis is still being limited by the (1) low photocatalytic reaction turnover time, (2) photocatalysts deactivation, (3) post-separation of the solid photocatalyst particles and (4) the need of rapid reactivation of the $TiO_2$ particles in a separate unit operation [20–23].

In this study, we developed and evaluated the photodegradation performance of a sequential batch annular slurry photoreactor (SB-ASP) system for the removal of antiepileptic drug CBZ from secondary municipal wastewater. The successful development and operation of semi-continuous photocatalytic wastewater treatment system is important, as it allows continuous treatment of larger wastewater volume without constant catalyst replenishment. CBZ is an antiepileptic drug that is usually used as sedative. From a toxicological point of view, this drug can produce serious toxic effects on the liver and hematopoietic system [24]. CBZ was used in this study, as a reaction surrogate tracer to observe the effects of complexity in wastewater effluents on its removal. Two immobilised photocatalysts were applied, namely: anatase titanate nanofibers and mesoporous $TiO_2$–K catalysts. Previously, both $TiO_2$ catalysts have shown an excellent photodegradation performance and recovery ability in a photoreactor system [21,25]. In this study,

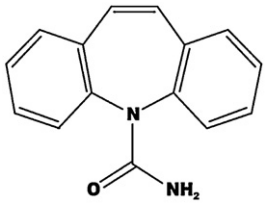


**Fig. 1.** The chemical structure of Carbamazepine (an antiepileptic drug).

a submerged microfiltration module with pore size of 0.2 μm was used in an annular slurry photoreactor (ASP) in order to retain the $TiO_2$ photocatalysts for semi-continuous operation of the SB-ASP system. The UV–Vis spectroscopic analysis via (1) high performance size exclusion chromatography (HPSEC) at 260 nm and (2) organic CBZ aromatic moieties at 280 nm were used to evaluate the change in the overall apparent molecular weight (AMW) profiles and the specific pharmaceutical indicator of CBZ. In addition, we also studied on the influence of nitrate ($NO_3^-$) and phosphate ($PO_4^{3-}$) ions on the photocatalytic reaction. With these, the impacts of effluent organic matter (EOM) and inorganic ions on the feasible photocatalytic degradation of CBZ compounds could be evaluated so as to determine their degree of mineralisation in the municipal wastewater matrix.

## 2. Experimental

### 2.1. Chemicals

Anatase particles (~325 mesh from Aldrich), titanium(IV) butoxide (tetrabutyl orthotitanate, purum grade ≥97% gravimetric, Sigma–Aldrich) and absolute ethanol (AR grade, Labserv Pronalys, Australia) were used as received. Raw kaolinite (K) clay materials were obtained from Unimin, Australia. CBZ (Sigma–Aldrich) was dissolved in the secondary treated biological wastewater. The chemical structure of CBZ is given in Fig. 1. Nitric acid ($HNO_3$) (AR grade, Aldrich), hydrochloric acid (HCl) (Labserv Pronalys, Australia) and sodium hydroxide (NaOH) (AR grade, Aldrich) were prepared to a designated concentration by the addition of Milli-Q water with 18.2 MΩ cm resistivity.

### 2.2. Preparation of photocatalysts

Anatase titanate nanofiber catalyst (TNC) was synthesized through a hydrothermal reaction between concentrated NaOH and $TiO_2$ and a post-synthesis ion exchange with HCl solution [26]. Specifically, 3 g of anatase particles was mixed with 80 mL of 10 M NaOH. The resultant suspensions were sonicated for 30 min and transferred into a PTFE container for autoclaving. The autoclave was maintained at hydrothermal temperature of 180 °C for 48 h. The precipitate (sodium titanate nanofibers) was recovered, washed with distilled water (to remove excess NaOH) and finally exchanged with $H^+$ (using a 0.1 M HCl solution) to produce hydrogen TNC. These products were repeatedly washed with distilled water until pH ~7 was reached. The hydrogen titanate product was dried at 80 °C for 12 h and then calcined at 700 °C for 3 h to yield anatase nanofibers. The resultant TNC fibrils were measured with thickness of 40–100 nm and length up to 30 μm long. Such fibril structure of TNC is expected to be easily filtered and possesses high photocatalytic efficiency owing to its thin fibril morphology that removes the mass transfer limitation.

The mesoporous $TiO_2$–K clay catalyst was synthesized via the modified two step sol–gel process [21]. Initially, 25 mL titanium n-butoxide precursor was hydrolysed by 30 mL of absolute ethanol. The hydrolysed mixture was then acid-catalysed with nitric acid

**Table 1**
The average wastewater quality for the primary influent from the WWTP and the secondary biological MBR treated effluent.

| Wastewater parameters | Primary influent to MBR | Secondary treated effluent from MBR |
|---|---|---|
| COD ($mg\,L^{-1}$) | 285–315 | 13.5–22.0 |
| $NO_3^-$ ($mg\,L^{-1}$) | 210–238 | 145.0–189.6 |
| $PO_4^{3-}$ ($mg\,L^{-1}$) | 21.7–23.8 | 19.9–20.3 |

of known molarity. In the following step, this acid-catalysed product was heterocoagulated with K-suspension of 10% (w/v) at 37 °C under constant stirring. The K clay particles in this instance are to provide a mesoporous platform for the deposition of $TiO_2$ sol, enabling ease of post-separation of catalyst particles after water treatment and high surface area for enhanced adsorption. After the heterocoagulation process, the products were filtered and washed repeatedly with distilled water up to three times to remove any excess chemical impurities. The filtrate cake was dried in a conventional oven at 65–70 °C for 3 h, before being fired at 600 °C. The resultant $TiO_2$–K catalyst was measured to have particle size distribution spans from 0.03 to 600 μm, with median size of 3.5 μm [21].

### 2.3. Sample preparation and wastewater collection

Primary wastewater sample was collected from the Glenelg WWTP, South Australia. This effluent was treated in a laboratory scale MBR system of 4 L capacity. A Zenon® hollow membrane (surface area of 0.047 $m^2$ and nominal pore size of 0.1 μm) was used in the sequential batch MBR, with a cycle of 15 min of wastewater recharge, 165 min of anoxic reaction, 60 min of aeration and followed by 240 min of combined aeration and filtration. The sludge retention time (SRT) used in the MBR was approximately 60 d. The treated effluents from the MBR were collected in a tank to ensure sufficient wastewater capacity for the subsequent photocatalytic integration treatment. Table 1 shows the wastewater quality of both the collected primary effluents from the WWTP and the secondary biological treated effluents from the MBR system.

CBZ was then dissolved in the effluents of the MBR system at 5 $mg\,L^{-1}$. Owing to the low solubility of CBZ, the mixture was magnetically stirred for 5 min and followed by sonication of 5 min. The final CBZ concentration in the dissolved phase was verified using the high performance liquid chromatography (HPLC) analysis. If a lower than 5000 $\mu g\,L^{-1}$ of CBZ concentration was attained, additional CBZ was dissolved to ensure the final CBZ concentration was as close to the targeted concentration as possible. Afterward, 3 L of this spiked effluent was mixed with either TNC or $TiO_2$–K catalyst of 1 $g\,L^{-1}$ for 30 min before being pumped through the SB-ASP system. Three different samplings were conducted both before the addition of CBZ and photocatalysts, and after 30 min mixing.

### 2.4. Setup of sequential batch annular slurry photoreactor

The SB-ASP used in this study was a modified photoreactor system based on our previous studies [20,25,27]. This SB-ASP was fabricated from stainless steel with a capacity of approximately 4.5 L and working volume of 3.6 L. The SB-ASP is operated as a three phase bubble column reactor, where the photocatalyst particles were suspended in the aqueous solution with the aid of air sparging. An air sparger with porosity of 45 μm was fitted to the detachable conical base of the vertical column. A low-intensity (11 W) UVC lamp was fitted annularly to the central axis of the column with the quartz thimble encapsulation to prevent direct fluid contact between the lamp and reaction mixture. Specific probes for in situ measurement of pH and DO were also fitted to monitor the properties change during the reaction. All the fluid connection lines were fitted with appropriate sized Tygon tubes for a complete SB-ASP system. To operate the SB-ASP mode, three different pumps were connected at the reactor inlet and outlet with the proper electronic timer adjustment. In this study, three different reaction schemes were proposed in one sequential batch reactor (SBR) cycle where initially (1) 3 L of the catalysts–water mixture will be recharged into column in a 0.5 h; followed by (2) the UVC photocatalytic reaction under certain post-determined time and finally (3) the discharge of 2 L of the reacted medium and co-catalyst reactivation in 1 h. It should be noted that after 1 h, the UVC lamp was programmed to be turned-off regardless of the capacity of the discharged volume. During the wastewater discharge phase, the microfiltration module was back-washed intermittently (10 s in every 10 min) to prevent the decline in filtration flux. In the following SBR cycle, 2 L of the fresh mixture will be recharged and mixed with the aged suspension. This procedure was repeated for three times to study of whether the catalysts were able to operate in such a mode or deactivated, resulting in the constant replacement of new photocatalysts. The experimental setup of the SB-ASP, together with the proposed SBR cycle is shown in Fig. 2.

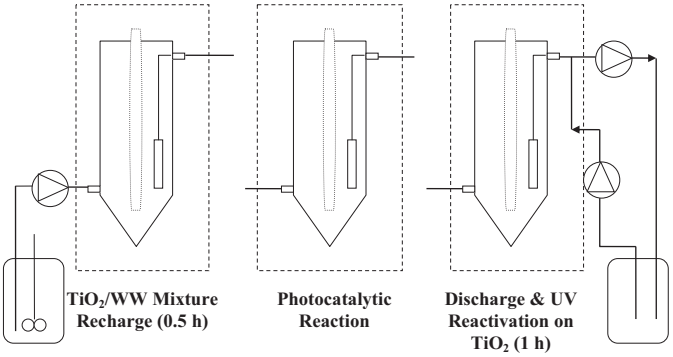


**Fig. 2.** Schematic for a SBR cycle with three different phases in a cycle. (1) $TiO_2$/wastewater (WW) recharges; (2) batch photocatalytic reaction and (3) discharge of 2/3 of original and UV reactivation on catalyst.

### 2.5. Analytical procedures

Four separate analytical methodologies were employed to monitor the removal of CBZ from the secondary treated effluents, to evaluate the subsequent effects of photocatalytic reaction on the CBZ intermediates and to determine the changes in the molecular weight profiles of the overall wastewater matrix.

The CBZ concentrations were analysed by a HPLC [Varian Prostar, Varian Microsorb-MW 100-5 C18 column (4.6 mm × 150 mm, 5 μm)] at a flowrate of 1.0 mL/min and UV absorbance detection at 254 nm. The mobile phase was methanol 60% plus ammonium acetate (10 mM) and acetic acid (5 mM). The injection volume was 20 μL. The UV–Vis absorbance of the sample was measured using a UV–Visible spectrophotometer (LIUV-201, Lambda Scientific Pty Ltd, Australia) equipped with a quartz cell having a path length of 1 cm. An absorbance at wavelength of 280 nm was conducted to detect the presence of possible aromatic pharmaceutical intermediates.

To investigate the changes in the AMW profile of the wastewater samples during photocatalysis, the samples were analysed using a coupling method of high-performance size exclusion chromatography (HPSEC) and UV detection [28]. Sample injection and separation were conducted with a Waters 2690 Alliance system with a temperature-controlled oven (30 °C) and a Shodex KW802.5 glycol functionalized silica gel column. Elution was monitored with a Waters 996 photodiode array detector (260 nm). Samples were

filtered through a 0.22 μm membrane filter prior to analysis and a sample volume of 100 μL was injected. The mobile phase was 0.02 M phosphate buffer at pH 6.8 adjusted to an ionic strength of 0.1 M with sodium chloride. The system was operated at isocratic conditions with an eluent flow rate of 1.0 mL/min. Polystyrene sulfonate standards (Polysciences, USA) with MW 4.6, 8, 18, and 35 kDa were used to calibrate the retention time response to AMW.

In order to determine the COD, an open reflux method was used where 2 mL of the sample was added into the low range 0–150 mg $L^{-1}$ COD reagent (Hach Lange GmbH, Germany) containing potassium dichromate ($K_2Cr_2O_7$) and subsequently heated for 2 h at 150 °C in a digestion reactor of DRB 200 (Hach Lange GmbH, Germany). The oxidizable organic compounds present will react with the $K_2Cr_2O_7$, and further reducing the dichromate ion to green chromic ion. Using this method, the amount of $Cr^{3+}$ produced was measured at the wavelength of 620 nm using a spectrophotometer DR4000 (Hach Lange GmbH, Germany) and the color intensity was correlated to the total oxidizable organic compounds and thus, giving the COD values.

As for the determination of inorganic $NO_3^-$ and $PO_4^{3-}$ in the wastewater matrix, similar manufactured reagents from Hach Lange GmbH, Germany were used. The total nitrogen was measured using the persulfate digestion method by Hach measurement kit (Hach Lange GmbH, Germany). The nitrogen that is present in the samples was converted into $NO_3^-$ through an alkaline persulfate digestion reagent and further heated at 105 °C for 30 min in the DRB 200 reactor. Then, the nitrate reacts with chromotropic acid under acid conditions to yield the final yellow complex that has an absorbance maximum at 410 nm. The final $NO_3^-$ values were obtained from the molecular weights conversion.

A vanadium molybdate spectrometry method (Hach Lange GmbH, Germany) was used to determine the $PO_4$-P concentration. In this method, the orthophosphate reacts with molybdate in an acid medium to produce a phosphomolybdate complex. When further reacted with vanadium, a yellow vanadomolybdophosphoric acid was formed. The intensity of the yellow color was used to correlate the phosphate concentration in the wastewater sample. To hydrolyse the condensed inorganic forms of phosphorous, the samples were pretreated with acid and heated 105 °C for 30 min in the DRB 200 reactor. Since the yellow color correlation gives the concentration in terms of total phosphorus, the final measurements in $PO_4^{3-}$ were converted using their corresponding molecular weights.

## 3. Results and discussion

### 3.1. Determination of sequential batch reaction time

To achieve this, we first investigated on the suitable range of SBR time to fit to the proposed scheme as in Section 2.4. Reaction times ranging from 0.5 to 4 h in 0.5 h increments were experimented, to find the optimum time between the COD, inorganic $NO_3^-$ and $PO_4^{3-}$ and AMW changes without CBZ spiked. The reason for not spiking CBZ in this instance is to serve as controlled experiments, so that the direct synergistic effect of the CBZ can be differentiated in the following section. Fig. 3 shows the normalised experimental outcomes on the effects of different SBR time on the key water parameters in the SB-ASP system using the two photocatalysts. Fig. 3 shows that the two photocatalysts used have different mechanisms and reactivity towards N atoms in the wastewater effluent. Fig. 3a suggests that the TNC fibrils have higher affinity for the conversion of N atoms that present in the effluent, leading to an increase in $NO_3^-$ concentration (24% increase) in a prolonged SBR time of 4 h. Low et al. [29,30] explained that in the photocatalytic oxidation of nitrogen, N will first converted to $NH_4^+$ and then to $NO_3^-$. The mesoporous $TiO_2$–K catalyst was found to have a lower conversion rate of N atoms to $NO_3^-$ as we deduced that most of the $NO_3^-$ was predominantly adsorbed (18% adsorbed at 4 h SBR time) onto the surface of the catalysts. Comparison of the two photocatalysts used suggested that such the gradual reduction in aqueous $NO_3^-$ with $TiO_2$–K might be owing to the $TiO_2$ immobiliser platform of K that posse a larger surface area for adsorption and higher tendency for ion exchange phenomena.

Similarly, Low et al. [29,30] demonstrated that the P atoms in wastewater matrices will be converted to $PO_4^{3-}$ during photocatalytic treatment. Connor and McQuillan [31] found that $PO_4^{3-}$ has a strong adsorption binds to the $TiO_2$ surface with further possibility to alter the surface chemistry of $TiO_2$ particles. The adsorption of $PO_4^{3-}$, however, is a strong function of pH and usually is elevated at a low pH owing to the electrostatic interaction. Fig. 3 shows that the $PO_4^{3-}$ was gradually reduced over prolonged SBR time by TNC photocatalysis, while $PO_4^{3-}$ adsorption in $TiO_2$–K catalyst shows similar trend but to a lesser adsorption extent. The $PO_4^{3-}$ concentration at 4 h SBR time using $TiO_2$–K only shows a 18% reduction, while 23% was observed in TNC fibrils. Two possible explanations for the higher $PO_4^{3-}$ removal efficiency in using TNC than $TiO_2$–K are that; (1) TNC has a higher affinity for strong adsorption binds to $PO_4^{3-}$, resulting in a lower measured $PO_4^{3-}$ ions concentration in the aqueous phase or (2) transformation of $PO_4^{3-}$ into different inorganic phosphate species in water.

Fig. 3 shows that the TNC has a higher affinity for organic mineralisation in the wastewater than the $TiO_2$–K. Over the 4 h SBR time, the TNC could reduce approximately 40% of dissolved organic content, while $TiO_2$–K catalyst could only achieve a 27% COD reduction at a photocatalyst concentration of 1 g $L^{-1}$. As discussed in our previous communication, the low affinity for organic mineralisation in $TiO_2$–K might be attributed to the low surface coverage of $TiO_2$ crystallites on the $TiO_2$–K catalyst [21]. In this study, however, we intend to keep both the photocatalyst loadings at 1 g $L^{-1}$ to facilitate the direct comparison with the standard Degussa P25 $TiO_2$ from other studies. The optimum aeration rates used in this study are different for both catalysts, and are highly dependent on the prior studies [20,25]. An aeration of 5.0 L/min and 7.5 L/min was used for TNC and $TiO_2$–K catalyst, respectively.

The COD measurements on the wastewater samples, accompanying with HPSEC UV 260 nm analysis (Fig. 4) show that both the photocatalysts are able to mineralise the dissolved organic components to different extent with varying SBR time. The HPSEC analysis (Fig. 4) shows that the EOM with AMW of >1–4 kDa was oxidized to form smaller organic compounds. The SBR time required to cause any physical and structural properties change for the EOM peak of 1–4 kDa appeared to be different for the two catalysts used, and found to vary between 1 and 2 h. It was interesting to note that the higher AMW EOM could be more easily degraded by the photo-oxidation than the lower AMW ones. This would prevent the formation of disinfection by-products and membrane fouling in the subsequent wastewater treatment stages. Considering all these changes in water parameters, the 2 h SBR time was selected to complete the SBR cycle of 0.5 h photocatalysts/wastewater mixture recharge, 2 h photocatalytic reaction and followed by 1 h wastewater discharge and simultaneous catalyst reactivation.

### 3.2. Photocatalytic degradation of Carbamazepine

In this section, CBZ of 5 mg $L^{-1}$ was spiked into the secondary biological treated wastewater as a collective representative of the pharmaceutical antiepileptic group that might present in wastewater. The extent of CBZ mineralisation in the wastewater was measured using four complementary analytical techniques of HPSEC $UV_{260\,nm}$, $UV_{280\,nm}$ and COD. The experimental data of the photocatalytic kinetics could be very useful to compare the

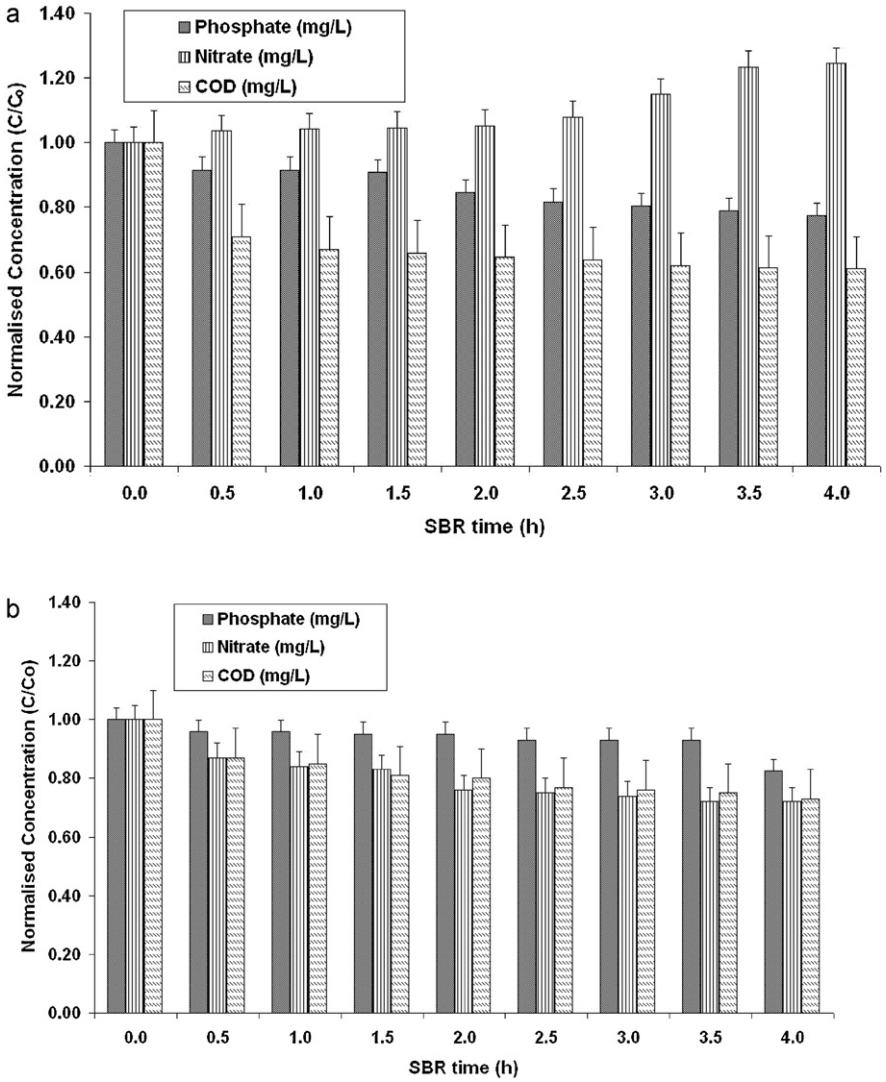


**Fig. 3.** Normalised photocatalytic effects on the wastewater parameters at different SBR time without CBZ spiked. (a) Using TNC fibrils; (b) using mesoporous $TiO_2$–K catalyst. Initial reaction conditions: 1 g $L^{-1}$ catalyst concentration and pH 7.40.

controlled experiments in the previous section, and therefore could further contribute to knowledge for the degradation of CBZ in wastewater.

Fig. 5 shows the photocatalytic oxidation of CBZ in secondary wastewater containing background EOM over three SBR cycles of 3.5 h each (10.5 h in total for 7 L treatment). From Fig. 5a, it can be seen that the TNC shows a high photoactivity in the first reaction cycle with a 70% COD reduction. When the CBZ concentration was measured in parallel, it was found that the high COD reduction does not entirely correspond to the CBZ degradation. The COD reduction was almost doubled when compared to the controlled experiment at 2 h SBR time without CBZ spiked. Such differences in COD might be attributed to the concurrent photocatalytic degradation of CBZ and its intermediates in the wastewater. This was further supported by the $UV_{280}$ measurement, which shows reduction in the characteristics peak for the aromatic organic fraction of the CBZ and its intermediates [32]. Only a 20% reduction in the density of the aromatic organic fraction of the CBZ was obtained from the $UV_{280}$ measurement. This means that the high COD reduction could be originated from the background EOM of the wastewater. The HPSEC chromatogram in Fig. 6a shows that the high AMW peaks of the EOM at AMW > 100 kDa were degraded with TNC photocatalysis, resulting in smaller AMW peaks that arise at 750 and 1050 Da, respectively. At this UV absorbance, the peak for CBZ which should be arising between 200 and 1000 Da seems to be insignificant. Also the results from the HPSEC chromatogram (Fig. 6a) indicated that the photocatalytic treatment has slightly shifted the AMW peaks towards smaller AMW. From all these data, it can be deduced that the TNC photocatalysis preferentially degrades the high molecular weights fraction of the EOM, forming smaller organic by-products and subsequently compete for the surface active sites with CBZ. High AMW fraction of the EOM is explained to be the preferential molecules to be attacked by the hydroxyl radicals, owing to the more reaction sites that promote TNC binding [28]. Huang et al. [33] also observed that the EOM has a very high adsorption affinity on $TiO_2$ particles with equilibrium reached in less than 5 min. Such preferential attack of high AMW fraction of the EOM rather than the CBZ has leaded to the partial oxidation of the CBZ compounds with 61% removal efficiency.

In situ pH measurement showed that there was a pH increase from initial value of 7.41 to 7.75. This pH rise might be due to the formation of partially oxidized CBZ intermediates of hydroxy- or chloro-natures. Doll and Frimmel [3] deducted on line the intermediates with CBZ degradation, and they found that 10,11-dihydro-CBZ-10,11-epoxide and 10,11-dihydro-CBZ were the main degradation products. When the same TNC catalysts were retained

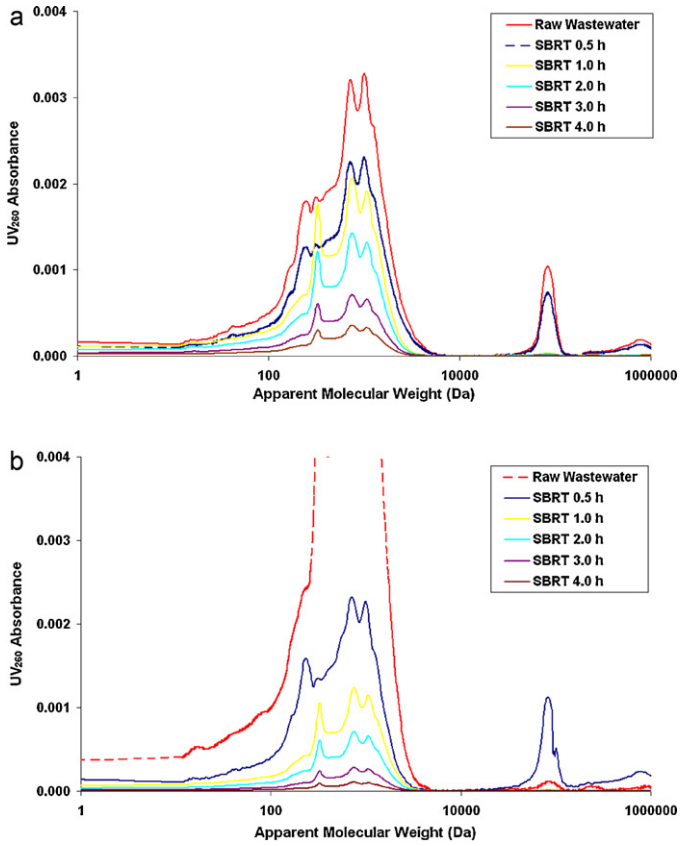


**Fig. 4.** HPSEC chromatogram at different SBR time without CBZ spiked. (a) Using TNC fibrils; (b) using mesoporous $TiO_2$–K catalyst.

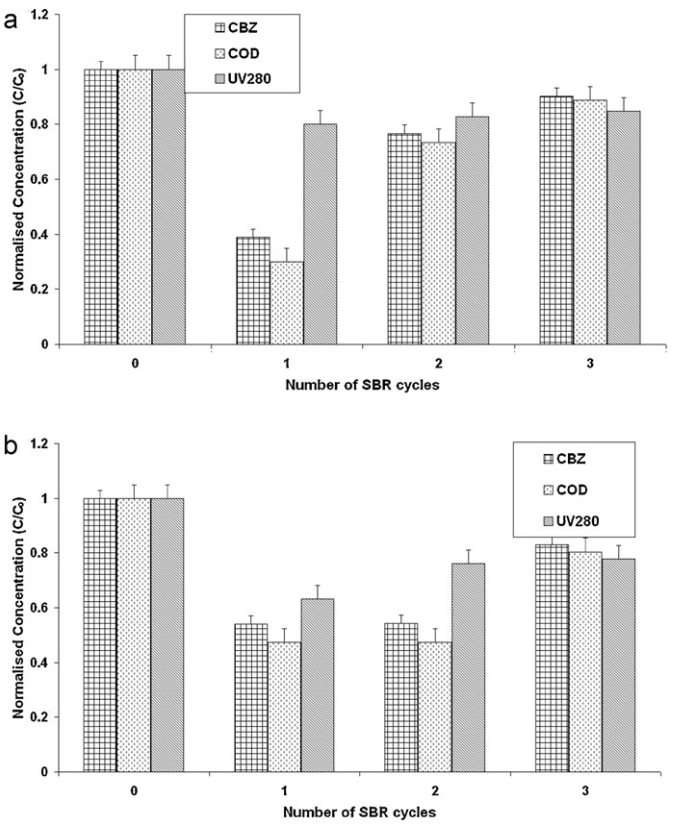


**Fig. 5.** Normalised photocatalytic oxidation effects on the reduction of CBZ, COD and $UV_{280}$ measurements in secondary wastewater over three SBR cycles. (a) Using TNC fibrils; (b) using mesoporous $TiO_2$–K catalyst. Initial reaction conditions: 1 g $L^{-1}$ catalyst concentration and pH 7.40.

for the following two reaction cycles with 2 L fresh wastewater added, it was observed that the photoactivity of the TNC gradually decreased with a COD reduction of 27% and 11% in the second and third reaction cycle, respectively (Fig. 5a). A similar declining trend was observed for the reduction in CBZ degradation (23% and 9%) and $UV_{280}$ (17% and 15%) measurements. These can be explained by catalyst deactivation by the $PO_4^{3-}$ ions in particular, and will be discussed in detail in following Section 3.3.

When the TNC photoactivity was compared with the composite nature of the $TiO_2$ crystallites on mesoporous $TiO_2$–K catalyst, it was seen that a high COD reduction rate was associated with the TNC fibrils. One of the reasons for such an inferior photoactivity in $TiO_2$–K is owing to the low surface-coverage of $TiO_2$–K catalysts with $TiO_2$ crystallites [21]. From Fig. 5b, however, the CBZ degradation by $TiO_2$–K catalysts as evidenced from both the HPLC and $UV_{280}$ measurements showed a more constant and photostable removal of CBZ over two consecutive reaction cycles. Fig. 6b shows the HPSEC chromatogram, indicating the similar removal in high AMW fraction removal of EOM. The higher stability associates with the $TiO_2$–K catalysis in SB-ASP mode over TNC might be attributed to the higher specific surface area of the mesoporous particles (35.24–15.70 $m^2$/g). The abrupt changes in the photocatalytic efficiency during the third reaction cycles with $TiO_2$–K might be owing to the low reaction turnover time, where its catalytic surface area was fully saturated and prevent the subsequent treatment of new contaminants in the fresh wastewater feed.

### 3.3. Effects of $NO_3^-$ and $PO_4^{3-}$ on SB-ASP performance

The effects of anions on the photo-degradation performance are inevitable as these anions are often associated with the complex matrices of wastewater or might evolve during the progress of the photocatalytic reaction. In this section, we evaluated the change in two important inorganic anions of $NO_3^-$ and $PO_4^{3-}$ during the photocatalytic oxidation of CBZ.

Previous studies on the photo-oxidation of organic compounds in the presence of $PO_4^{3-}$ have concluded that such anion remains strongly adsorbed on the $TiO_2$ surface under a wide pH range, and further inhibits its photoactivity [34,35]. Further in situ internal reflection infrared spectroscopy study by Connor and McQuillan [31] confirmed such strong binding of $PO_4^{3-}$ on the $TiO_2$ surface, where they concluded that the $PO_4^{3-}$ shows a fast adsorption and slow desorption process. On contrary, $NO_3^-$ was reported to have minimal inhibition of the $TiO_2$ surface but may act as an inner filter that UV screening the photocatalyst particles [35].

Controlled experiments in Section 3.1 without CBZ revealed that in 2 h SBR time, the $PO_4^{3-}$ removal is higher in TNC (15%) than the $TiO_2$–K (5%) catalyst used. During the first SB-ASP cycle with CBZ, the $PO_4^{3-}$ removal for both TNC and $TiO_2$–K catalyst is of 21% and 25%, respectively (Fig. 7). The subsequent second and third SB cycles, however, showed an abrupt reduction in $PO_4^{3-}$ removal for both $TiO_2$ catalysts. Connor and McQuillan [31] explained that there are specific sites on the surface of $TiO_2$ that binds only $PO_4^{3-}$ and $CO_3^{2-}$. This means that the $PO_4^{3-}$ inhibition does not entirely affect the CBZ degradation but causes only a partial reduction in total surface sites. These were evidenced from the unparallel CBZ and COD removal efficiency with its $PO_4^{3-}$ removal at both second and third SB cycles, even the $PO_4^{3-}$ removal abruptly dropped after the first cycle. The $PO_4^{3-}$ reduction during the second cycle for both TNC and $TiO_2$–K catalysts was 3% and 10%, respectively, while approximately 1% removal was obtained for both catalysts in the third SB cycle. Simultaneously, the CBZ degradation for the second and third cycles using TNC and $TiO_2$–K was 23% and 46% in the second cycle

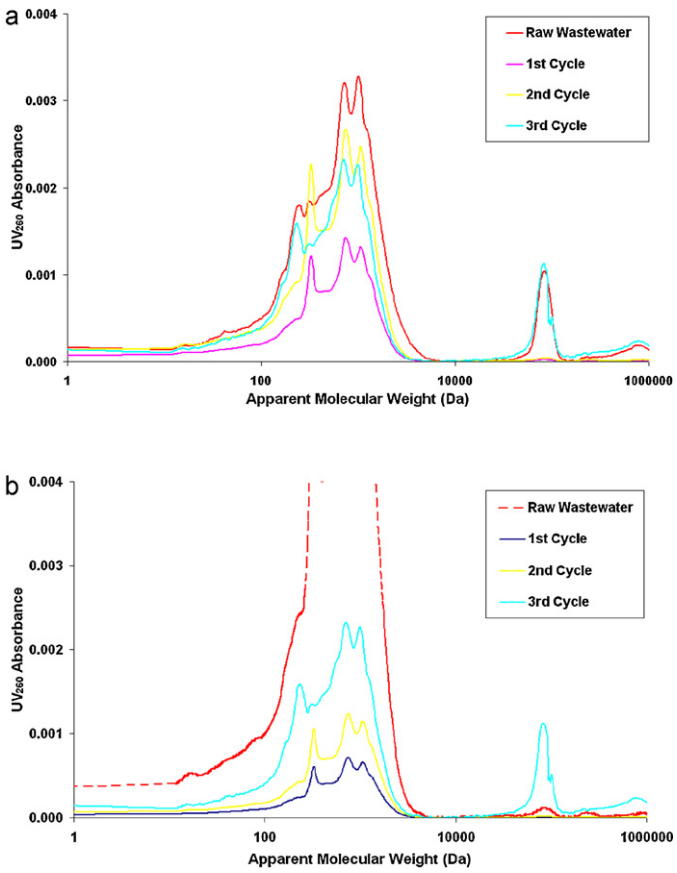


**Fig. 6.** HPSEC chromatogram at different SBR times with 5 mg $L^{-1}$ CBZ spiked. (a) Using TNC fibrils; (b) using mesoporous $TiO_2$–K catalyst.

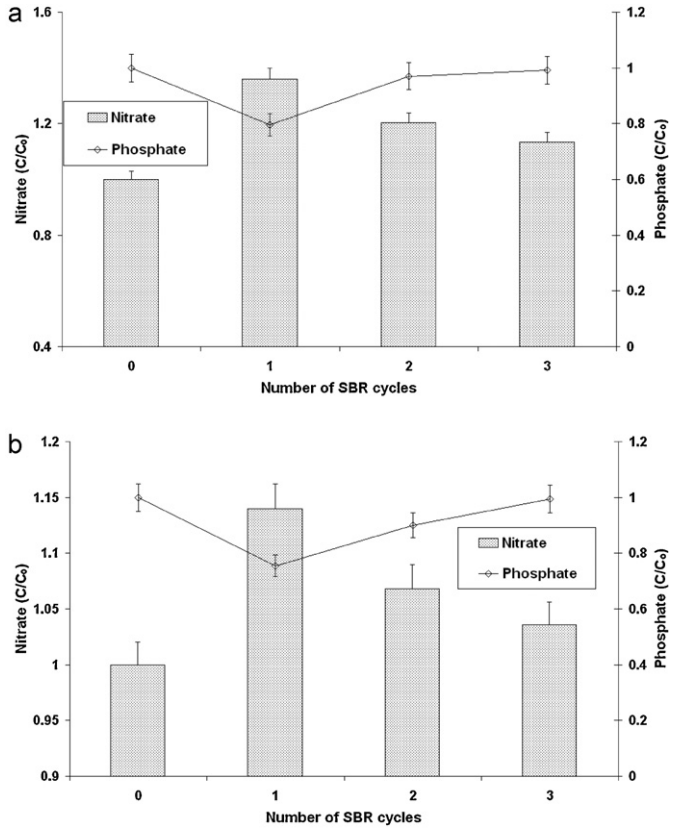


**Fig. 7.** Changes in $NO_3^-$ and $PO_4^{3-}$ concentration during the SB-ASP operation over three SBR cycles.

and 10% and 17% in the third cycle, respectively. Thus, it can be concluded that the anionic $PO_4^{3-}$ in the wastewater has a partial effect on the photocatalyst fouling and deactivation for subsequent use. However, the phosphate fouling does not proportionally reduce the photoactivity as it can be seen from the phosphate uptake (adsorption) at each SB cycles with the CBZ and COD removal efficiency.

The independent effects of $NO_3^-$ on the photo-oxidation of CBZ could not be qualitatively evaluated in this study. It was, however, interesting to note that the $NO_3^-$ concentration increased after each SB cycles using the two catalysts (Fig. 7). The extent of the $NO_3^-$ evolution in this case was seen to strongly correlate to the amount of CBZ degraded during the 2 h reaction cycles. As CBZ is amine functional compound, the increase in $NO_3^-$ in this case might be owing to the partial photooxidation of CBZ that releases the N atoms into the wastewater effluent. Prolonged oxidation of the N atoms during the photocatalytic reaction will contribute to an increase in the overall $NO_3^-$ concentration. In this instance, the measurement of $NO_3^-$ can be used as a relative indicator for the extent of CBZ degradation during the photooxidation process. From the SB-ASP operation using both catalysts, it can be concluded that the overall $NO_3^-$ evolution rate was higher in TNC over $TiO_2$–K used (Fig. 7).

## 4. Conclusion

The possible integration of a microfiltration module into the ASP for semi-continuous degradation of CBZ in secondary wastewater via the SBR operation mode has been successfully demonstrated where no residual $TiO_2$ particles were detected at the treated effluent stream. From this work, it can be shown that the SB-ASP operation with immobilised $TiO_2$ catalysts is a promising approach to enhance the degradation of persistent pharmaceuticals while retaining the photocatalysts for continuous advanced wastewater treatment. It is expected that such SB-ASP system could be operated in conjunction with a biological treatment process, so as to establish an integrated chemical-biological treatment process for wastewater reclamation and reuse, due to the combined removal capacity, better water quality and lower process operation costs.

When the pharmaceutical CBZ was degraded in the presence of high molecular weight EOM in wastewater, preferential attack on the EOM was found to be one of the key reasons that lower the degradation efficiency of CBZ. Other than this, the $PO_4^{3-}$ in the wastewater was also found to have a detrimental effect of photocatalyst fouling and deactivation on both $TiO_2$ catalysts used. However, we found that the $PO_4^{3-}$ fouling is site specific and does not completely retard the photoactivity of the catalysts used. Also, the $NO_3^-$ evolution rate measured from the degradation was found to be strongly correlated to the CBZ oxidation. In conclusion, the TNC fibril has shown higher photoactivity and affinity for the CBZ degradation, while the mesoporous $TiO_2$–K catalysts show higher adsorption capacity and photostability over the three assessed cycles for each catalyst. Further works need to be carried out to get a better understanding of the effects of different wastewater constituents on the degradation of pharmaceutical CBZ in complex wastewater effluent. This information is important for the optimization of the operation of SB-ASP (i.e. SBR cycle time, catalyst dosage, aeration rate) for a better treatment performance.

## Acknowledgements

The authors would like to thank Ms. Vipasiri Vimonses and the technical assistances and Professor Huai Yong Zhu for providing the TNC fiber samples. This work was supported by the Australian Research Council Linkage Grant (LP0562153) and the Australian Water Quality Centre, SA Water Corporation, through the Water

Environmental Biotechnology Laboratory (WEBL) at the University of Adelaide.

## References


[1] M. Klavarioti, D. Mantzavinos, D. Kassinos, Removal of residual pharmaceuticals from aqueous systems by advanced oxidation processes, Environ. Int. 35 (2009) 402–417.

[2] K. Kümmerer, The presence of pharmaceuticals in the environment due to human use – present knowledge and future challenges, J. Environ. Manage. 90 (2009) 2354–2366.

[3] T.E. Doll, F.H. Frimmel, Removal of selected persistent organic pollutants by heterogeneous photocatalysis in water, Catal. Today 101 (2005) 195–202.

[4] T.E. Doll, F.H. Frimmel, Photocatalytic degradation of carbamazepine, clofibric acid and iomeprol with P25 and Hombikat UV100 in the presence of natural organic matter (NOM) and other organic water constituents, Water Res. 39 (2005) 403–411.

[5] T.E. Doll, F.H. Frimmel, Cross-flow microfiltration with periodical back-washing for photocatalytic degradation of pharmaceutical and diagnostic residues – evaluation of the long term stability of the photocatalytic activity of $TiO_2$, Water Res. 39 (2005) 847–854.

[6] N. Muir, J.D. Nichols, J.M. Clifford, J. Skyes, Comparative bioavailability of aspirin and acetaminophen following single dose administration of soluble and plain tablets, Curr. Med. Res. Opin. 13 (1997) 491–500.

[7] T. Heberer, U. Dünnbier, C. Reilich, H.J. Stan, Detection of drugs and drug metabolites in groundwater samples of drinking water treatment plant, Fresenius Environ. Bull. 6 (1997) 438–443.

[8] T.A. Ternes, Occurrence of drugs in German sewage treatment plants and rivers, Water Res. 32 (1998) 3245–3260.

[9] A. Putschew, S. Wischnack, M. Jekel, Occurrence of triiodinated X-ray contrast agents in the aquatic environment, Sci. Total Environ. 255 (2000) 129–134.

[10] F. Sacher, F.T. Lange, H.J. Brauch, I. Blankenhorn, Pharmaceuticals in groundwaters analytical methods and results of a monitoring program in Baden-Württemberg, Germany, J. Chromatogr. A 938 (2001) 199–210.

[11] P.D. Anderson, V.J. D'Aco, P. Shanahan, S.C. Chapra, M.E. Buzby, V.L. Cunningham, B.M. Duplessie, E.P. Hayes, F.J. Mastracco, N.J. Parke, J.C. Rader, J.H. Samuelian, B.W. Schwab, Screening analysis of human pharmaceutical compounds in US surface waters, Environ. Sci. Technol. 38 (2004) 838–859.

[12] J. Radjenović, M. Petrović, D. Barceló, Fate and distribution of pharmaceuticals in wastewater and sewage sludge of the conventional activated sludge (CAS) and membrane bioreactor (MBR) treatment, Water Res. 43 (2009) 831–841.

[13] N. Klameth, L. Rizzo, S. Malato, M.I. Maldonado, A. Agüera, A.R. Fernández-Alba, Degradation of fifteen emerging contaminants at microg L(−1) initial concentrations by mild solar photo-Fenton in MWTP effluents, Water Res. 44 (2010) 545–554.

[14] T.A. Ternes, M. Meisenheimer, D. McDowell, F. Sacher, H.J. Brauch, B. Haist-Gulde, G. Preuss, U. Wilme, N. Zulei-Seibert, Removal of pharmaceuticals during drinking water treatment, Environ. Sci. Technol. 36 (2002) 3855–3863.

[15] S. Esplugas, D.M. Bila, L.G.T. Krause, M. Dezotti, Ozonation and advanced oxidation technologies to remove endocrine disrupting chemicals (EDCs) and pharmaceuticals and personal care products (PPCPs) in water effluents, J. Hazard. Mater. 149 (2007) 631–642.

[16] R. Rosal, A. Rodríguez, J.A. Perdigón-Melón, M. Mezcua, M.D. Hernando, P. Letón, E. García-Calvo, A. Agüera, A.R. Fernández-Alba, Removal of pharmaceuticals and kinetics of mineralization by $O_3/H_2O_2$ in a biotreated municipal wastewater, Water Res. 42 (2008) 3719–3728.

[17] V. Belgiorno, L. Rizzo, D. Fatta, C.D. Rocca, G. Lofrano, A. Nikolaou, V. Naddeo, S. Meric, Review on endocrine disrupting-emerging compounds in urban wastewater: occurrence and removal by photocatalysis and ultrasonic irradiation for wastewater reuse, Desalination 215 (2007) 166–176.

[18] F. Méndez-Arriaga, S. Esplugas, J. Giménez, Photocatalytic degradation of non-steroidal anti-inflammatory drugs with $TiO_2$ and simulated solar irradiation, Water Res. 42 (2008) 585–594.

[19] G. Laera, M.N. Chong, B. Jin, A. Lopez, An integrated MBR-$TiO_2$ photocatalysis process for the removal of Carbamazepine from simulated pharmaceutical industrial effluent, Bioresour. Technol. 102 (2011) 7012–7015.

[20] M.N. Chong, S. Lei, B. Jin, C. Saint, C. Chow, Optimisation of an annular photoreactor process for degradation of Congo red using a newly synthesized titania impregnated kaolinite nano-photocatalyst, Sep. Purif. Technol. 67 (2009) 355–363.

[21] M.N. Chong, V. Vimonses, S. Lei, B. Jin, C. Chow, C. Saint, Synthesis and characterisation of novel titania impregnated kaolinite nano-photocatalyst, Microporous Mesoporous Mater. 117 (2009) 233–242.

[22] M.J. Benotti, B.D. Stanford, E.C. Wert, S.A. Snyder, Evaluation of a photocatalytic reactor membrane pilot system for the removal of pharmaceuticals and endocrine disrupting compounds from water, Water Res. 43 (2009) 1513–1522.

[23] S. Malato, P. Fernández-Ibáñez, M.I. Maldonado, J. Blanco, W. Gernjak, Decontamination and disinfection of water by solar photocatalysis: recent overview and trends, Catal. Today 147 (2009) 1–59.

[24] R. Molinari, F. Pirillo, V. Loddo, L. Palmisano, Heterogeneous photocatalytic degradation of pharmaceuticals in water by using polycrystalline $TiO_2$ and a nanofiltration membrane reactor, Catal. Today 118 (2006) 205–213.

[25] M.N. Chong, B. Jin, H.Y. Zhu, C.W.K. Chow, C. Saint, Application of H-titanate nanofibers for degradation of Congo red in an annular slurry photoreactor, Chem. Eng. J. 150 (2009) 49–54.

[26] H. Zhu, X. Gao, Y. Lan, D. Song, Y. Xi, J. Zhao, Hydrogen titanate nanofibers covered with anatase nanocrystals: a delicate structure achieved by the wet chemistry reaction of the titanate nanofibers, J. Am. Chem. Soc. 126 (2004) 8380–8381.

[27] M.N. Chong, B. Jin, C.W.K. Chow, C.P. Saint, A new approach to optimise an annular slurry photoreactor system for the degradation of Congo red: statistical analysis and modelling, Chem. Eng. J. 152 (2009) 158–166.

[28] S. Liu, M. Lim, R. Fabris, C. Chow, M. Drikas, R. Amal, $TiO_2$ photocatalysis of natural organic matter in surface water: impact on trihalomethanes and haloacetic acid formation potential, Environ. Sci. Technol. 42 (2008) 6218–6223.

[29] G.K.C. Low, S.R. McEvoy, R.W. Matthews, Formation of nitrate and ammonium ions in titanium dioxide mediated photocatalytic degradation of organic compounds containing nitrogen atoms, Environ. Sci. Technol. 25 (1991) 460.

[30] G.K.C. Low, M. Zhang, Degradation of hazardous organics in water by titanium dioxide mediated photocatalytic oxidation, in: Proc. Emerging Technologies for Hazardous Waste Management, vol. 2, Atlanta, Georgia, 1992, pp. 507–510.

[31] P.A. Connor, A.J. McQuillan, Phosphate adsorption onto $TiO_2$ from aqueous solutions: an in situ internal reflection infrared spectroscopic study, Langmuir 15 (1999) 2916–2921.

[32] L. Rizzo, S. Meric, M. Guida, D. Kassinos, V. Belgiorno, Heterogeneous photocatalytic degradation kinetics and detoxification of an urban wastewater treatment plant effluent contaminated with pharmaceuticals, Water Res. 43 (2009) 4070–4078.

[33] X. Huang, M. Leal, Q. Li, Degradation of natural organic matter by $TiO_2$ photocatalytic oxidation and its effect on fouling of low-pressure membranes, Water Res. 42 (2008) 1142–1150.

[34] M. Kerzhentsev, C. Guillard, J.M. Herrmann, P. Pichat, Photocatalytic pollutant removal in water at room temperature: case study of the total degradation of the insecticide fenitrothion (phosphorothioic acid O,O-dimethyl-O-(3-methyl-4-nitro-phenyl) ester), Catal. Today 27 (1996) 215–220.

[35] M. Abdullah, G.K.C. Low, R.W. Matthews, Effects of common inorganic anions on rates of photocatalytic oxidation of organic carbon over illuminated titanium dioxide, J. Phys. Chem. 94 (1990) 6820–6825.